Supporting Information

Enhanced cyclability of Li-O_2 battery with cathodes of Ir and MnO_2 supported on well defined TiN array

Limin Leng [a,b], Jing Li [a], Xiaoyuan Zeng [a], Xinlong Tian [a], Huiyu Song [a], Zhiming Cui [a,], Ting Shu [a], Haishui Wang [a], Jianwei Ren [c], Shijun Liao [a,*]*

[a]*The Key Laboratory of Fuel Cell Technology of Guangdong Province, School of Chemistry and Chemical Engineering, South China University of Technology, Guangzhou 510641, China.*

[b]*Sunwoda Electronic Co., Ltd, Shenzhen, Guangdong 518100, China*

[c]*HySA Infrastructure Centre of Competence, Materials Science and Manufacturing, Council for Scientific and Industrial Research (CSIR). PO Box 395, Pretoria 0001, South Africa.*

* Corresponding author Fax: +86 20 87113586. E-mail address: chsjliao@scut.edu.cn
* Corresponding author Fax: +86 20 87113586. E-mail address: cuizm26@gmail.com

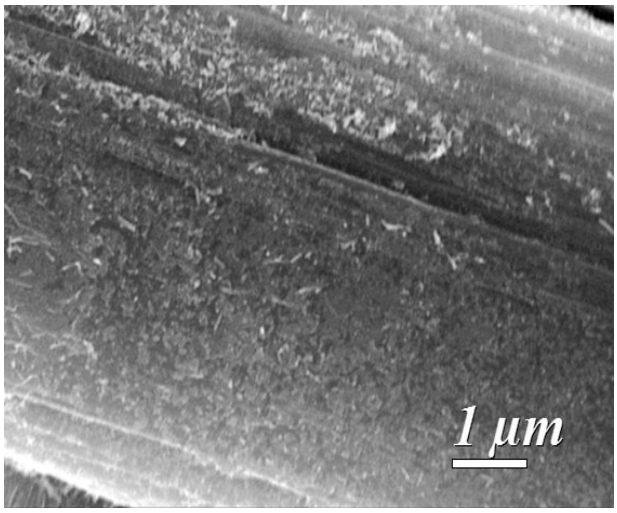

Fig. S1 SEM image of the sample after seed layer is generated on the carbon paper.

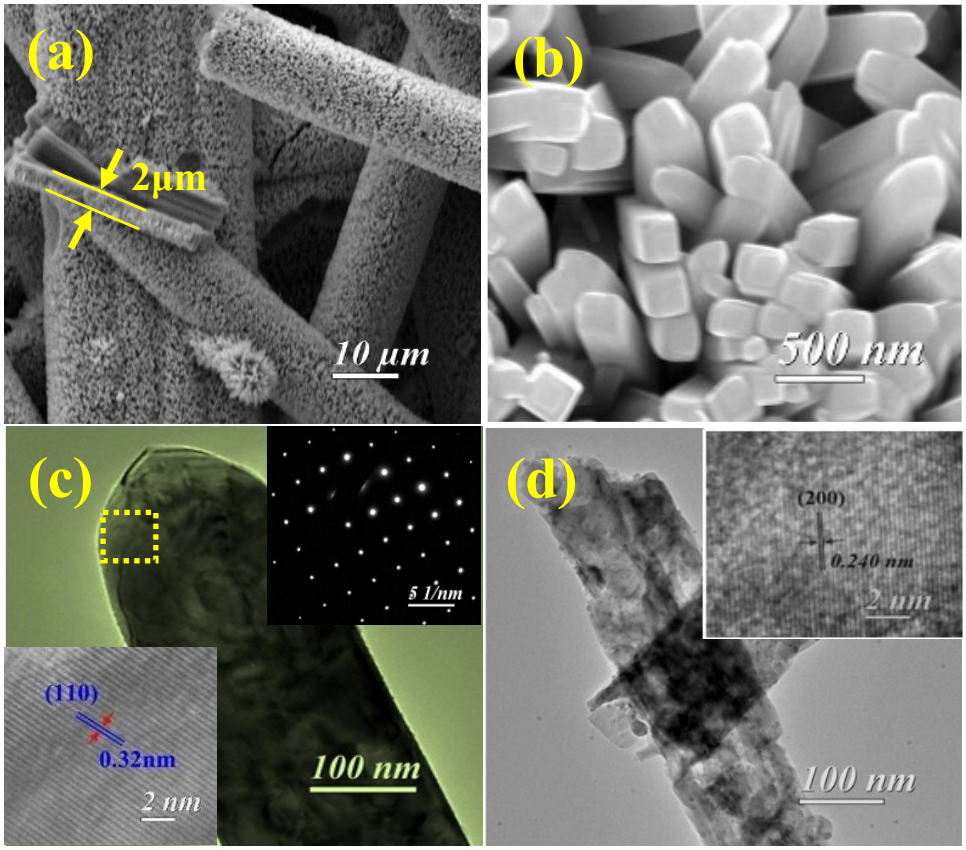

Fig. S2 SEM and magnified SEM images of (a, b) TiO_2/CP; TEM images of (c) TiO_2 nanorod, and (d) TiN nanorod catalysts (the insets are the SAED pattern and HR-TEM images).

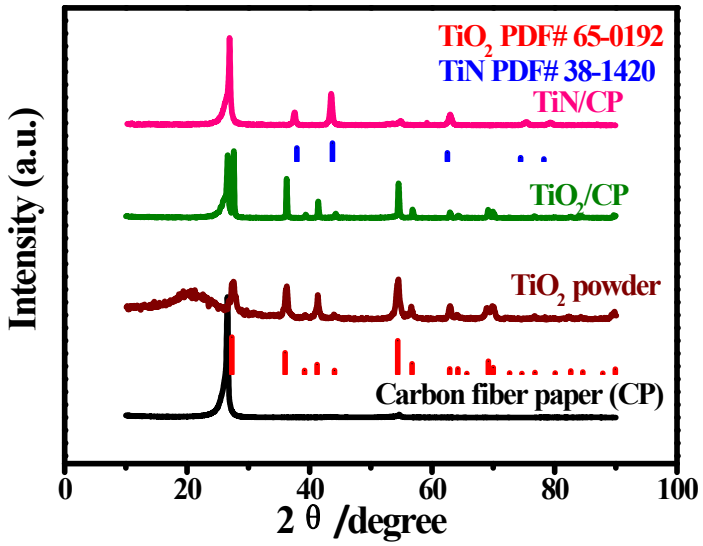

Fig. S3 XRD patterns of the as-prepared various cathodes.

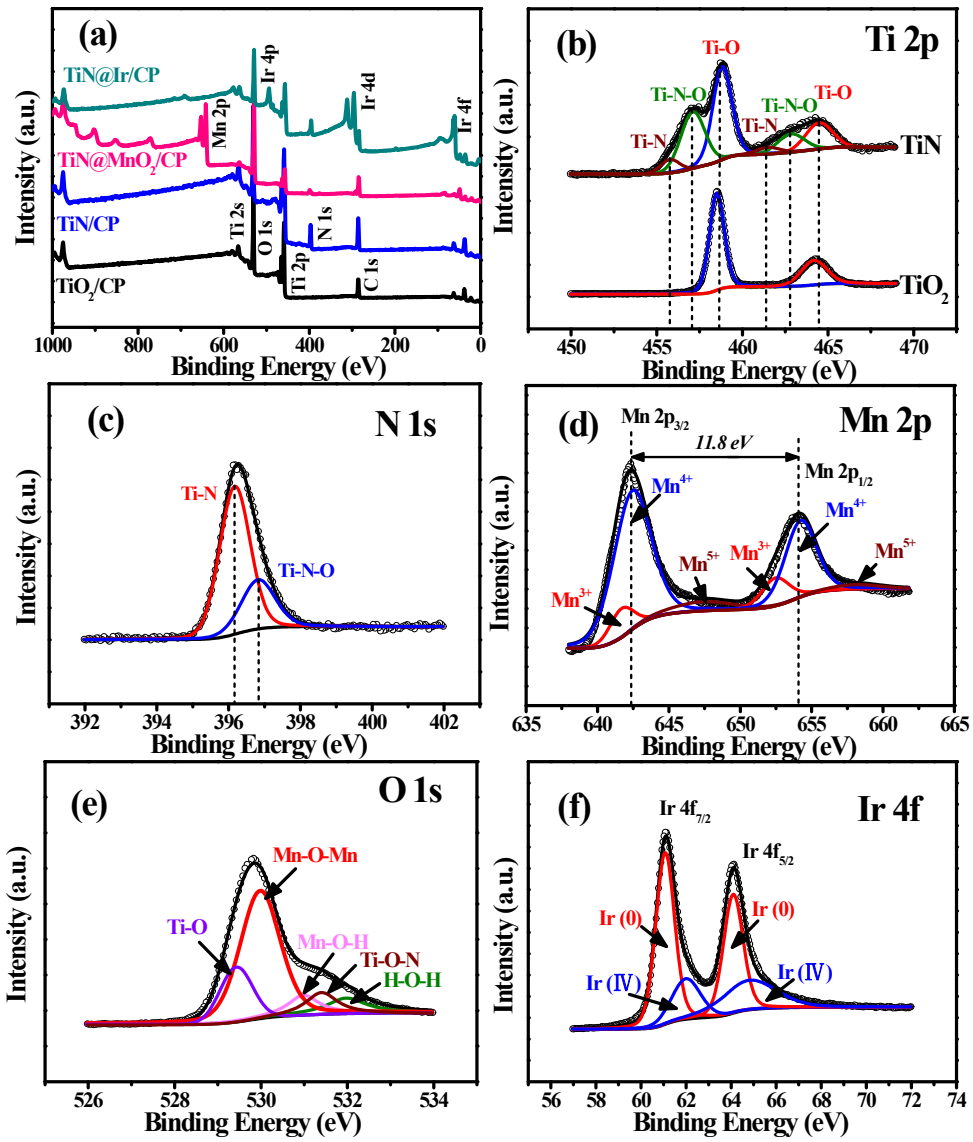

Fig. S4 XPS spectrum of (a) the as-prepared electrodes and b) Ti 2p, (c) N1s, (d) Mn 2p, (e) O 1s and (f) Ir 4f.

The XPS survey spectra of TiN/CP cathode exhibits the N 1s peak with a bond energy around 396 eV (Figure S3c), confirming the N substituting O atom in the crystal lattice and formation of the Ti–N. Multiple peaks are evolved at lower binding energies in the Ti 2p spectra as depicted in Fig. S3b, which can be assigned to be Ti−N ($2p_{3/2}$ = 455.8 eV and $2p_{1/2}$ = 461.53 eV), Ti−N−O ($2p_{3/2}$ = 457.12 eV and $2p_{1/2}$ = 463.1 eV), and Ti−O ($2p_{3/2}$ = 458.84 eV and $2p_{1/2}$ = 464.5 eV)[1-3]. Moreover, N 1s spectrum (Fig. S3c) was analyzed by deconvolution method, the characteristic peaks at binding energies of 396.18 and 396.83 eV correspond to Ti–N and Ti–N–O peaks,

respectively. Fig. S4d and e display the Mn 2p and O1s spectra for the TiN@MnO_2/CP cathode, respectively. The Mn 2p spectrum presents two main peaks located at 642.45 and 654.25 eV, being assigned to Mn $2p_{3/2}$ and Mn $2p_{1/2}$ with a spin-energy separation of 11.8 eV, which are in accordance with the previous reports on MnO_2[4, 5]. In the O 1s region, there are three peaks with the binding energies of 529.8, 531.0 and 532.0 eV. The sharp peak located at 529.8 eV is for O element in Mn–O–Mn oxide, and other two peaks at 531.0 and 532.0 eV correspond to O element in hydroxide (Mn–O–H) and water (H–O–H)[4, 6]. The high resolution XPS spectrum of Ir 4f (Fig. S3f) exhibits dominating Ir (0) $4f_{5/2}$ and Ir (0) $4f_{7/2}$ with fractional Ir (IV) $4f_{5/2}$ and Ir (IV) $4f_{7/2}$ suggesting a certain degree of surface oxidation, which is a common phenomenon among metal nanoparticles.

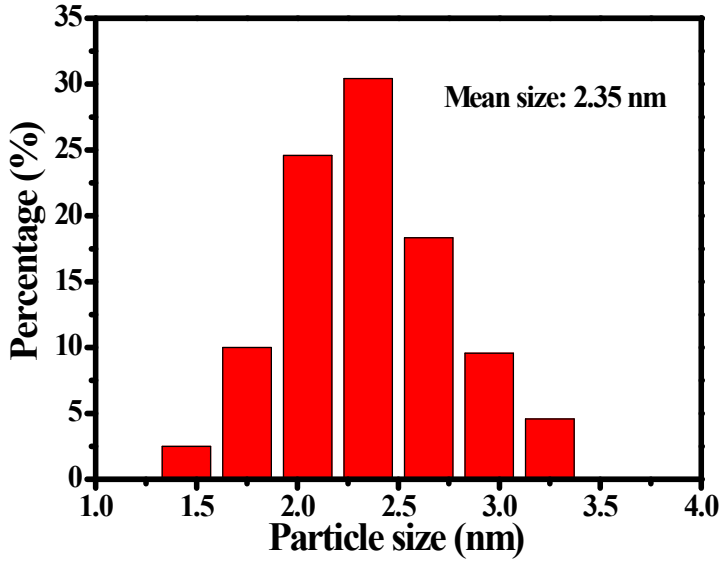

Fig. S5 The particle size distribution of iridium nanoparticles in TiN@Ir catalyst.

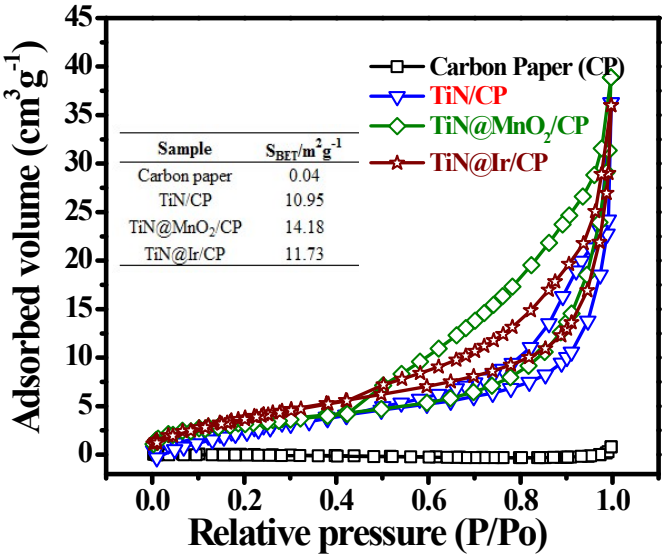

Fig. S6 N_2 adsorption-desorption isotherms of various cathodes.

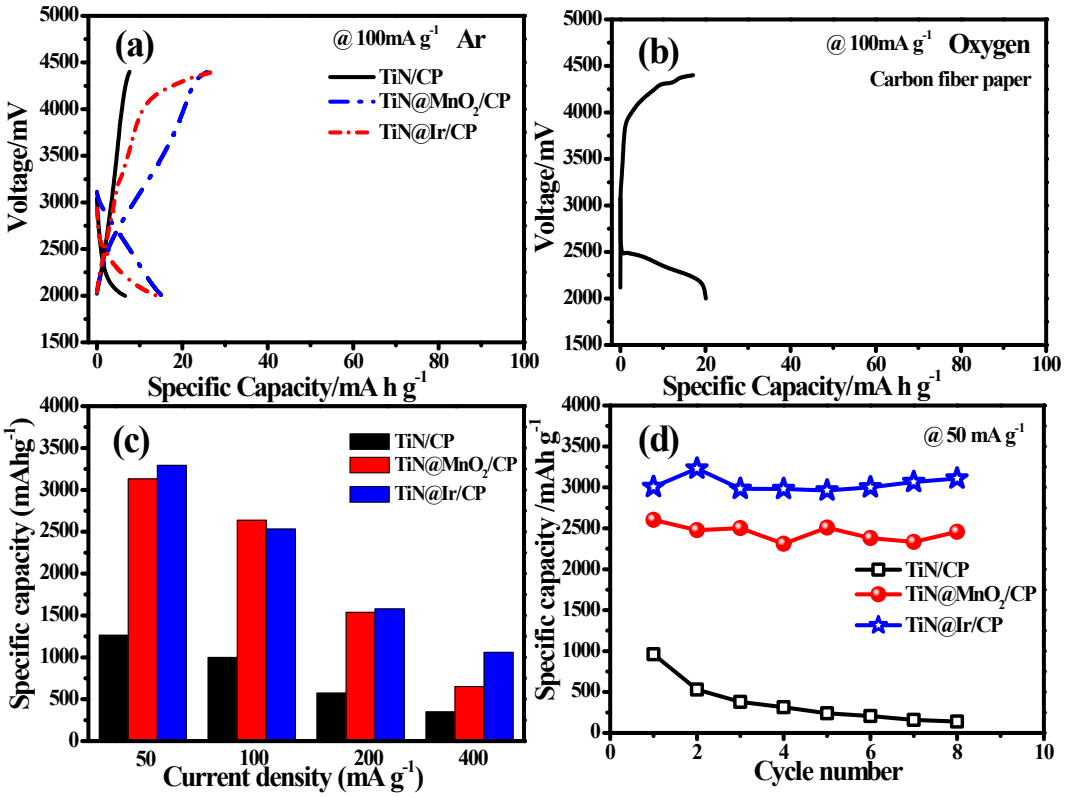

Fig. S7 The discharge-charge curves of the various electrodes at 100 mA g^{-1} under (a) Ar and (b) O_2 atmosphere; (c) Specific capacities and (d) cycling performance of Li–O_2 batteries with various cathodes.

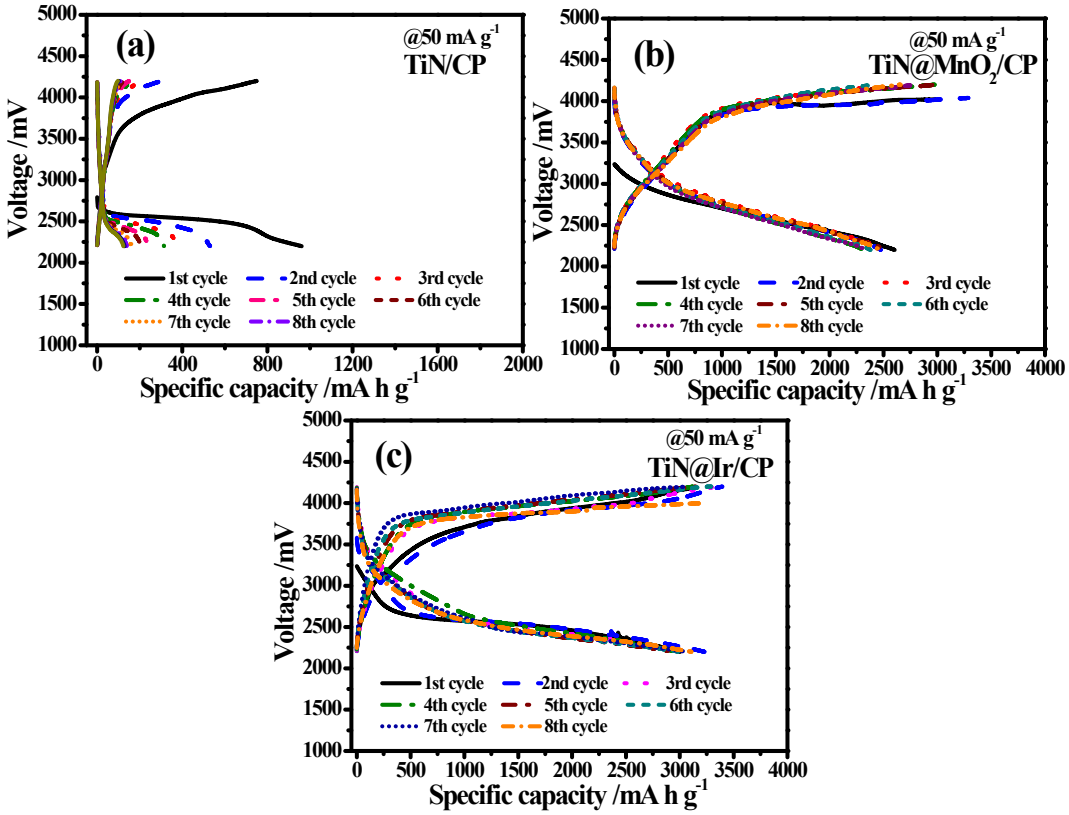

Fig. S8 Discharge/charge curves of Li–O_2 batteries with (a) TiN/CP, (b) TiN@MnO_2/CP and (c) TiN@Ir/CP cathodes at 50 mA g^{-1}.

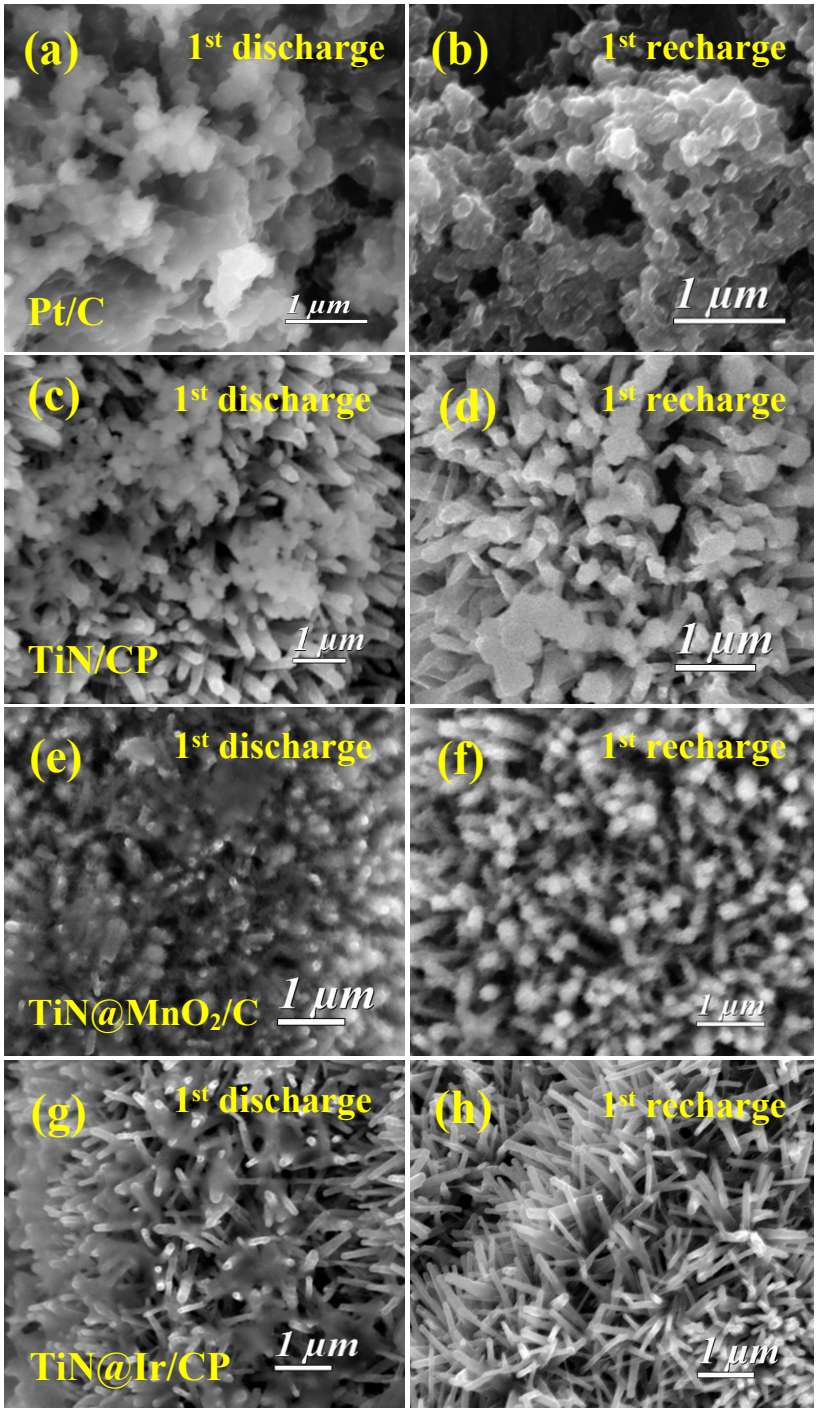

Fig. S9 SEM images of (a, b) Pt/C; (c, d) TiN/CP; (e, f) TiN@MnO_2/CP and (g, h) TiN@Ir/CP cathodes after the first fully discharged (a, c, e, g) and recharged (b, d, f, h) process at a current density of 100 mA g^{-1}.

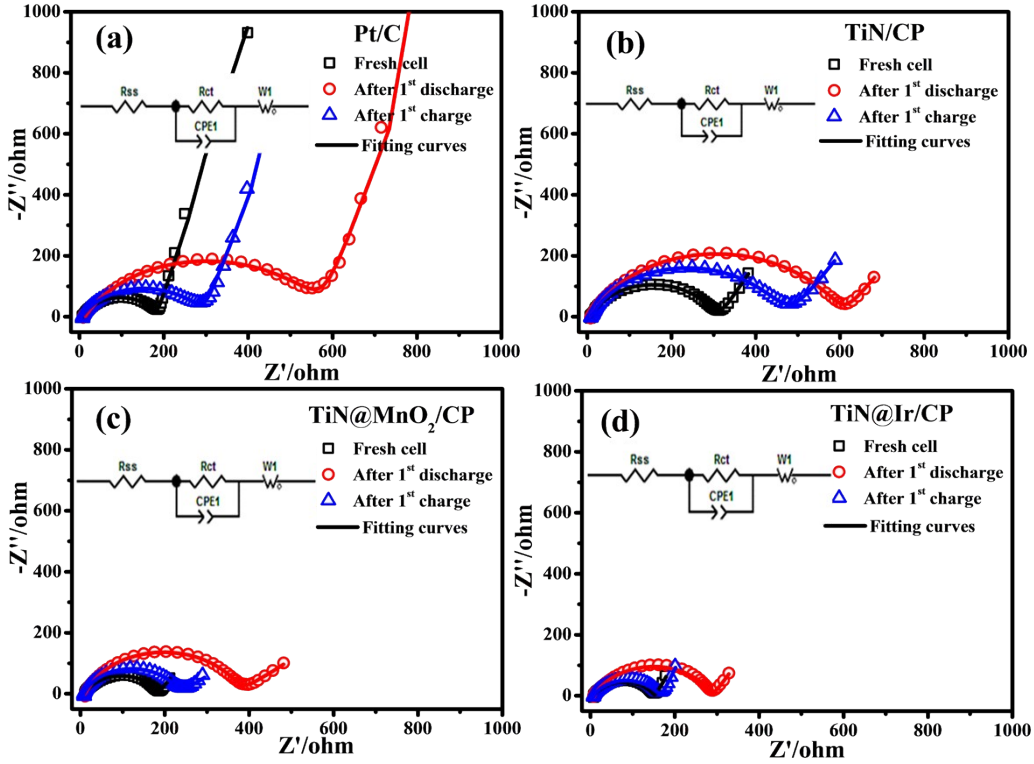

Fig. S10 Electrochemical impedance spectra (EIS) of Li–O_2 batteries with various cathodes (a) Pt/C, (b) TiN/CP, (c) TiN@MnO_2/CP and (d) TiN@Ir/CP at the first fully discharged and recharged.

Table S1 Values of the fitting parameters evaluated from the equivalent circuit with various cathodes at the first fully discharged/charged.

Catalytic cathodes	State	Rss /ohm	Rct /ohm	CPE-T /μF	CPE-P	W1-R /ohm	W1-T /F	W1-P
Pt/C	Fresh	10.01	173.5	10.87	0.80	5694	14.24	0.85
	discharged	12.75	564.7	16.96	0.72	7328	16.54	0.84
	recharged	9.37	285.6	21.21	0.72	4829	16.48	0.83
TiN/CP	Fresh	12.29	279.3	7.58	0.80	76.23	0.584	0.35
	discharged	14.47	573.2	9.34	0.78	72.04	0.526	0.33
	recharged	12.92	422.9	8.37	0.79	154.9	1.03	0.34
TiN@MnO_2/CP	Fresh	10.45	173.1	14.52	0.77	25.79	0.20	0.34
	discharged	8.93	355.1	7.32	0.82	31.4	0.04	0.23
	recharged	8.15	223.1	10.07	0.80	47.0	0.92	0.22
TiN@Ir/CP	Fresh	7.31	145.5	16.45	0.76	6.62	0.02	0.37
	discharged	8.82	278.9	13.49	0.78	67.58	0.52	0.35
	recharged	7.46	152	16.45	0.77	29.58	0.26	0.39

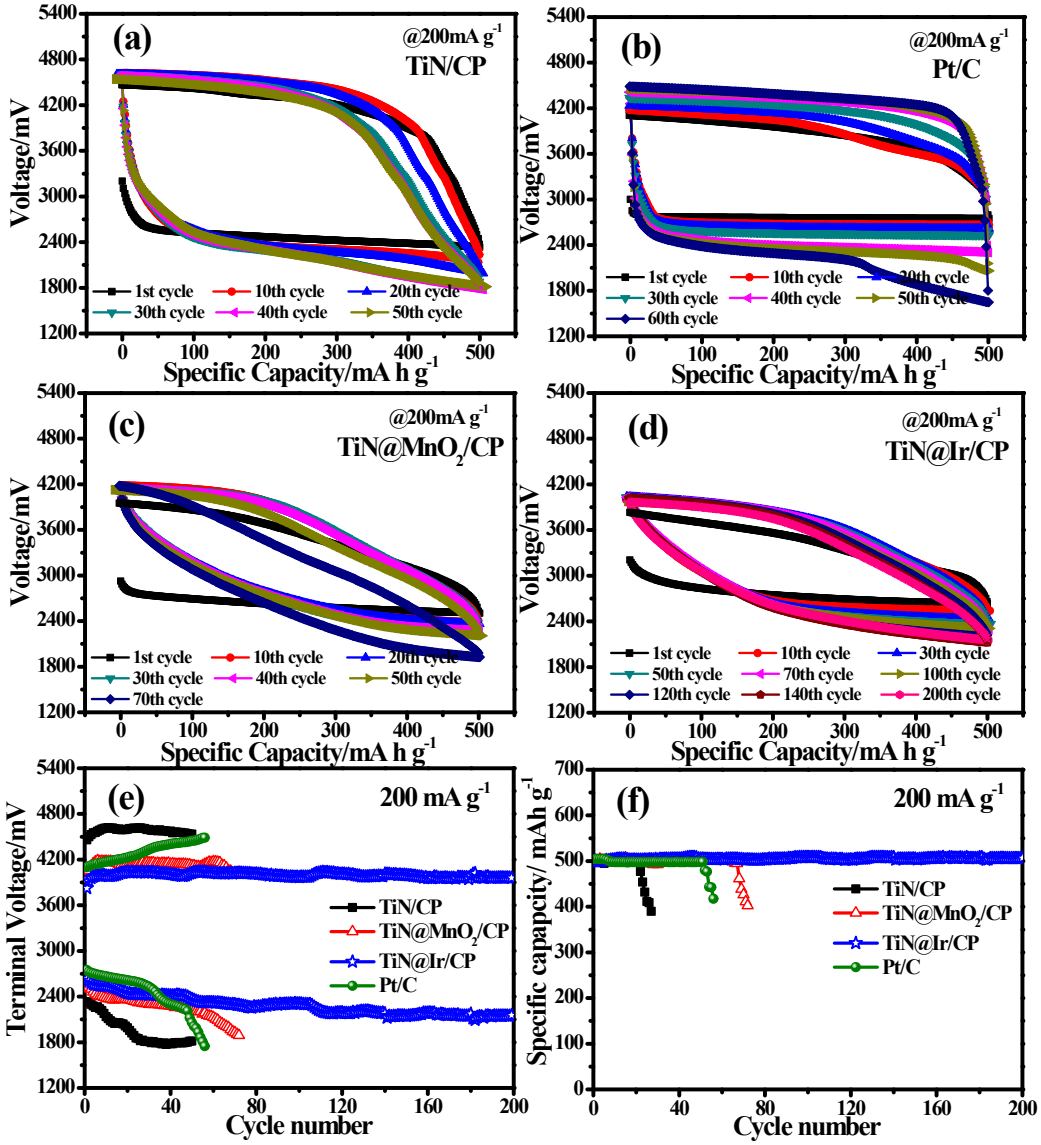

Fig. S11 The cycling performance of Li–O_2 batteries with the (a) TiN/CP, (b) Pt/C, (c) TiN@MnO_2/CP and (d) TiN@Ir/CP electrodes at 200 mA g^{-1} with a limited capacity of 500 mA h g^{-1}; (e) the terminal voltage and (f) capacities of discharge with various cathodes vs. cycle number.

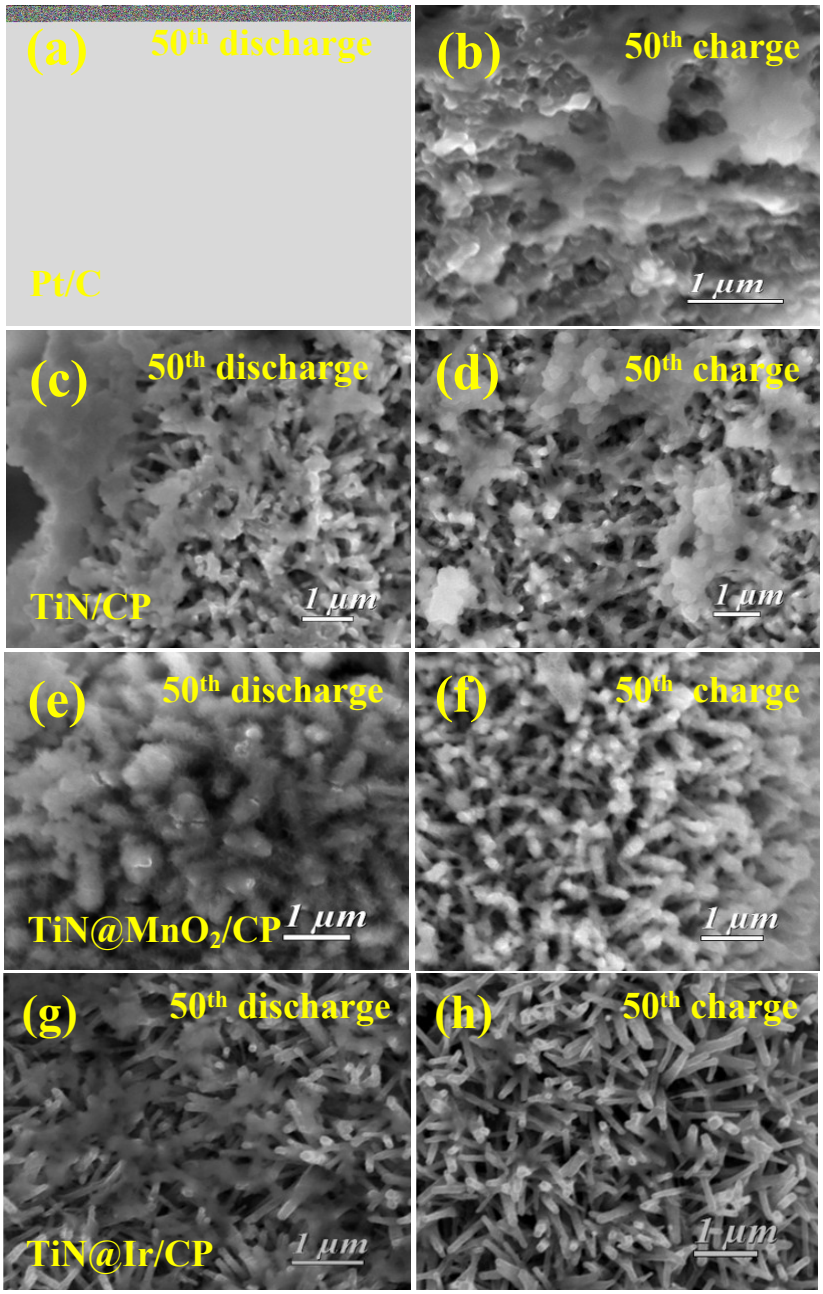

Fig. S12 SEM images of Li–O_2 batteries with the (a, b) Pt/C; (c, d) TiN/CP; (e, f) TiN@MnO_2/CP and (g, h) TiN@Ir/CP cathodes after the 50th discharged (a, c, e, g) and charged (b, d, f, h) at 100 mA g^{-1} with a fixed capacity of 500 mA h g^{-1}.

References

1. X. C. a. C. Burda, *J. Phys. Chem. B*, 2004, 108, 15446-15449.
2. J. Z. Ye Cong, Feng Chen and Masakazu Anpo, *J. Phys. Chem. C*, 2007, 111, 6976-6982.
3. B. Avasarala, T. Murray, W. Li and P. Haldar, *Journal of Materials Chemistry*, 2009, 19, 1803-1805.
4. T. B. a. D. B. l. Mathieu Toupin, *Chem. Mater.*, 2004, 16, 3184-3190.
5. A. L. Reddy, M. M. Shaijumon, S. R. Gowda and P. M. Ajayan, *Nano letters*, 2009, 9, 1002-1006.
6. M. C. a. M. Ishikawa, *Journal of The Electrochemical Society*, 2000, 147, 2246-2251.